PHYSICAL REVIEW B **80**, 100502(R) (2009)

Disorder-sensitive superconductivity in the doped iron silicide superconductor $(Lu_{1-x}R_x)_2Fe_3Si_5$ (R=Sc, Y, and Dy)

Tadataka Watanabe, Hiroki Sasame, Hiroaki Okuyama, Kouichi Takase, and Yoshiki Takano
Department of Physics, College of Science and Technology (CST), Nihon University, Chiyoda-ku, Tokyo 101-8308, Japan
(Received 30 June 2009; published 8 September 2009)

We studied the effect of nonmagnetic and magnetic impurities on superconductivity in $Lu_2Fe_3Si_5$ by small-amount substitution of the Lu site and investigated structural, magnetic, and electrical properties of nonmagnetic $(Lu_{1-x}Sc_x)_2Fe_3Si_5$, $(Lu_{1-x}Y_x)_2Fe_3Si_5$, and magnetic $(Lu_{1-x}Dy_x)_2Fe_3Si_5$. The rapid depression of T_c by nonmagnetic impurities in accordance with the increase in the residual resistivity reveals the strong pair breaking dominated by disorder.

DOI: 10.1103/PhysRevB.80.100502 PACS number(s): 74.20.Rp, 74.62.Dh, 74.70.Dd, 74.25.Jb

Recent discovery of high-T_c superconductivity in the FeAs systems has shed a brilliant light on Fe-based substances as a rich vein of new exotic superconductors.[1] In addition to deeper studies of the FeAs systems, it is also indispensable to explore the exotic superconductivity in Fe-based substances other than the FeAs family. Ternary iron silicide $Lu_2Fe_3Si_5$ is a non-FeAs-family superconductor discovered in 1980.[2] This compound crystallizes in the tetragonal $Sc_2Fe_3Si_5$-type structure consisting of a quasi-one-dimensional iron chain along the c axis and quasi-two-dimensional iron squares parallel to the basal plane.[3] The superconductivity occurs at T_c=6.0 K, which is exceptionally high among the Fe-based compounds other than the FeAs family. According to Mössbauer experiments, Fe atoms in $Lu_2Fe_3Si_5$ carry no magnetic moment.[4] Taking into account the absence of superconductivity in the isoelectronic $Lu_2Ru_3Si_5$ and $Lu_2Os_3Si_5$,[5] Fe 3d electrons in $Lu_2Fe_3Si_5$ should play significant role in the occurrence of the superconductivity.

To unveil the pairing mechanism of the exotic superconductivity, it is crucial to determine the superconducting gap function. In $Lu_2Fe_3Si_5$, recent measurements of specific heat[6] and penetration depth[7] reported the evidence for two-gap superconductivity, similar to MgB_2 which is considered to be a two-gap s-wave superconductor.[8] The Josephson effect suggested the spin-singlet superconductivity in $Lu_2Fe_3Si_5$.[9] On the other hand, past experimental studies in $Lu_2Fe_3Si_5$ reported peculiar superconducting properties which are different from MgB_2: for instance, a power-law temperature dependence of specific heat below T_c (Ref. 10) and a remarkable depression of T_c by nonmagnetic impurities.[11,12] In addition, recent photoemission spectroscopy in the superconducting state observed the gap opening without distinct coherence peaks implying the nodal structure,[13] in contrast to the two coherence peaks clearly observed in MgB_2.[14] It should be noted that "cleanliness" in terms of the electron mean-free path is necessary and common conditions to the occurrence of the multigap and the non-s-wave (e.g., p- or d-wave) superconductivities, and thus these are co-occurrable in the "clean" system.[15] In the multigap system, we should also take into account another possibility of the extended s-wave ($s_\pm$-wave) superconductivity in which the sign of the order parameter changes between the different Fermi sheets. This has recently been supposed as a possible pairing symmetry for the FeAs systems, both theoretically[16] and experimentally.[17] The recent and the past experimental reports in $Lu_2Fe_3Si_5$ require studies on verification of the sign reversal of the superconducting order parameter.

The effect of impurity scattering is sensitive to the phase of the superconducting gap function.[18] The s-wave superconductivity is robust against nonmagnetic impurities while strongly suppressed by magnetic impurities. On the contrary, the non-s-wave even-parity superconductivity, with the presence of nodes in the gap, is sensitive to both nonmagnetic and magnetic impurities. The $s_\pm$-wave superconductivity, with the sign change of the order parameter between the different Fermi sheets, is expected to exhibit the impurity effects similar to the non-s-wave even-parity superconductivity.[19]

This Rapid Communication reports study of nonmagnetic and magnetic impurity effects on the superconductivity of $Lu_2Fe_3Si_5$ by small-amount substitution of nonmagnetic Sc, Y, and magnetic Dy for Lu. Earlier, a brief account of magnetic susceptibility studies in the solid solutions $(Lu_{1-x}R_x)_2Fe_3Si_5$ (R=Sc, Y, and Dy-Tm) was reported in which T_c was depressed with R substitutions.[12] The present study particularly takes interest in the effect of disorder on the superconductivity in $Lu_2Fe_3Si_5$, and we study the correlation between T_c and the residual resistivity. We investigate structural, magnetic, and electrical properties of polycrystalline $(Lu_{1-x}R_x)_2Fe_3Si_5$ (R=Sc, Y, and Dy). In addition, we investigate anisotropy of electrical resistivity in a high-purity $Lu_2Fe_3Si_5$ single crystal, motivations of which are described later with the results.

Polycrystals of $(Lu_{1-x}Sc_x)_2Fe_3Si_5$, $(Lu_{1-x}Y_x)_2Fe_3Si_5$ (x =0–0.07 and 1), and $(Lu_{1-x}Dy_x)_2Fe_3Si_5$ (x=0–0.05 and 1) were prepared by arc melting stoichiometric amounts of high-purity elements in Zr-gettered Ar atmosphere. To ensure the sample homogeneity, the arc melting was repeated with turning over the melted ingot for more than ten times. A high-purity single crystal of $Lu_2Fe_3Si_5$ was grown by the floating-zone method. The polycrystalline and the single-crystalline samples were annealed at 1050 °C for 2 weeks. Powder x-ray diffraction patterns showed that all the samples crystallize in the $Sc_2Fe_3Si_5$-type structure without any additional peak. dc magnetic susceptibilities and electrical resistivities were measured by using the Quantum Design Physical Property Measurement System.

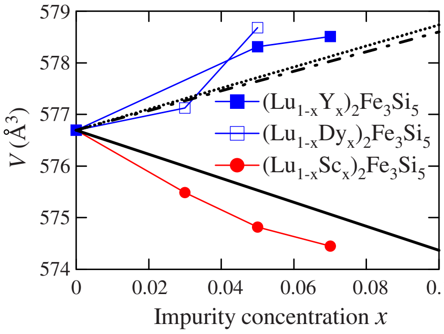

FIG. 1. (Color online) The unit-cell volumes of $(Lu_{1-x}Sc_x)_2Fe_3Si_5$, $(Lu_{1-x}Y_x)_2Fe_3Si_5$, and $(Lu_{1-x}Dy_x)_2Fe_3Si_5$ as functions of impurity concentration x. Solid, dotted, and dashed lines denote the Vegard's law in $(Lu_{1-x}Sc_x)_2Fe_3Si_5$, $(Lu_{1-x}Y_x)_2Fe_3Si_5$, and $(Lu_{1-x}Dy_x)_2Fe_3Si_5$, respectively.

Figure 1 depicts the unit-cell volumes of $(Lu_{1-x}Sc_x)_2Fe_3Si_5$, $(Lu_{1-x}Y_x)_2Fe_3Si_5$, and $(Lu_{1-x}Dy_x)_2Fe_3Si_5$ as functions of the impurity concentration x. The Vegard's law lines expected from the unit-cell volumes of $Lu_2Fe_3Si_5$ (576.7 Å), $Sc_2Fe_3Si_5$ (553.4 Å), $Y_2Fe_3Si_5$ (597.1 Å), and $Dy_2Fe_3Si_5$ (595.7 Å) are also presented. It is evident that all the samples obey Vegard's law: the unit-cell volume increases with x in $(Lu_{1-x}Y_x)_2Fe_3Si_5$ and $(Lu_{1-x}Dy_x)_2Fe_3Si_5$, while it decreases with x in $(Lu_{1-x}Sc_x)_2Fe_3Si_5$. These results ensure that Y, Sc, and Dy atoms are properly introduced as impurities into the parent $Lu_2Fe_3Si_5$ phase with the Lu-site substitutions.

Figure 2 depicts the magnetic susceptibilities of the polycrystalline $Lu_2Fe_3Si_5$, $(Lu_{1-x}Y_x)_2Fe_3Si_5$ ($x=0.05$), $(Lu_{1-x}Sc_x)_2Fe_3Si_5$ ($x=0.07$), and $(Lu_{1-x}Dy_x)_2Fe_3Si_5$ ($x=0.03$ and 0.05) as functions of temperature with $H=10\,000$ Oe. $(Lu_{1-x}Dy_x)_2Fe_3Si_5$ exhibits the pronounced Curie tail due to the inclusion of the magnetic Dy atoms, in contrast to the nonmagnetic behavior in $Lu_2Fe_3Si_5$, $(Lu_{1-x}Y_x)_2Fe_3Si_5$, and $(Lu_{1-x}Sc_x)_2Fe_3Si_5$. Here, we estimate the concentration of Dy atoms in the present $(Lu_{1-x}Dy_x)_2Fe_3Si_5$ from the Curie-Weiss behavior. The magnetic moment of Dy atom in $Dy_2Fe_3Si_5$ estimated from the Curie-Weiss behavior is $\mu=10.4\mu_B$, which is close to the free-ion value ($\mu=10.6\mu_B$). Using $\mu=10.4\mu_B$, the Curie-Weiss analysis tells us that 3.07% and 4.92% of Lu atoms are substituted by Dy atoms in the $x=0.03$ and 0.05 samples of $(Lu_{1-x}Dy_x)_2Fe_3Si_5$, respectively, ensuring that the Dy atoms are properly doped as magnetic impurities in these samples. The inset to Fig. 2 displays the low-temperature magnetic susceptibilities with $H=10$ Oe, exhibiting the diamagnetism due to the superconducting transition. For all the samples applied in the present study, the onset of the diamagnetism coincides with that of the zero-resistance transition, and we adopt these onset temperatures as T_c.

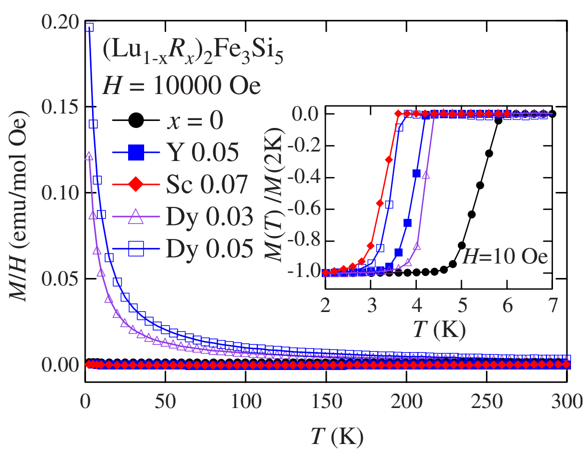

FIG. 2. (Color online) The magnetic susceptibilities of polycrystalline $Lu_2Fe_3Si_5$, $(Lu_{1-x}Y_x)_2Fe_3Si_5$ ($x=0.05$), $(Lu_{1-x}Sc_x)_2Fe_3Si_5$ ($x=0.07$), and $(Lu_{1-x}Dy_x)_2Fe_3Si_5$ ($x=0.03$ and 0.05) as functions of temperature with $H=10\,000$ Oe. Inset shows the superconducting transitions with $H=10$ Oe.

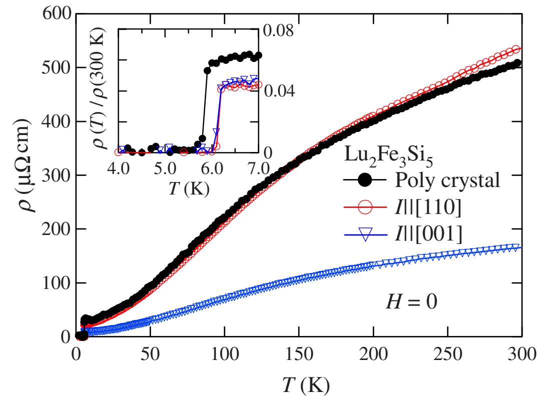

FIG. 3. (Color online) The electrical resistivity of single-crystalline ($I\|[001]$ and $I\|[110]$) and polycrystalline $Lu_2Fe_3Si_5$ as functions of temperature. Inset shows the low-temperature resistivities normalized to the values at 300 K.

The electrical resistivities of single-crystalline and polycrystalline $Lu_2Fe_3Si_5$ are presented in Fig. 3 as functions of temperature. Superconducting transition occurs at $T_c=6.1$ and 5.8 K in the single-crystalline and the polycrystalline samples, respectively. For the single crystal, we investigate the anisotropy of the resistivity with the current I parallel and perpendicular to the crystal c axis, $I\|[001]$ and $I\|[110]$, respectively. As shown in Fig. 3, the c-axis resistivity ρ^c is less than one third of the in-plane resistivity ρ^{ab} in the whole temperature range. The normal-state residual resistivities are $\rho_0^c=7.0$ $\mu\Omega$ cm and $\rho_0^{ab}=22$ $\mu\Omega$ cm, respectively. At 300 K, the polycrystalline resistivity ρ^p exhibits an intermediate value between the single-crystalline ρ^c and ρ^{ab}, $\rho^c(300\text{ K}) < \rho^p(300\text{ K}) < \rho^{ab}(300\text{ K})$. $\rho^p(300\text{ K})$ is close to but smaller than $\rho^{ab}(300\text{ K})$, indicating that ρ^p is a weighted average of ρ^c and ρ^{ab} which dominantly picks up ρ^{ab} as a component rather than ρ^c. As the temperature is lowered below $\sim$140 K, ρ^p becomes slightly larger than ρ^{ab}. The normal-state residual resistivity of the polycrystal is $\rho_0^p=30$ $\mu\Omega$ cm, which is larger than ρ_0^c and ρ_0^{ab}, indicating that the polycrystal is "dirty" compared to the single crystal in terms of the electron mean-free path.

The inset to Fig. 3 shows the low-temperature resistivities ρ^c, ρ^{ab}, and ρ^p normalized to the values at 300 K, $\rho(T)/\rho(300\text{ K})$. It is evident that ρ^c and ρ^{ab} exhibit almost identical $\rho(T)/\rho(300\text{ K})$: for the residual resistivities ρ_0^c and ρ_0^{ab}, $\rho_0/\rho(300\text{ K})=0.04$. Since $\rho(T)/\rho(300\text{ K})$ cancels the

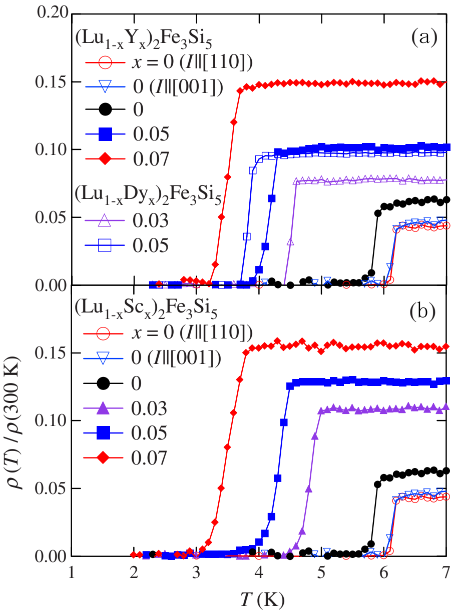

FIG. 4. (Color online) Temperature dependence of the normalized resistivity $\rho(T)/\rho(300\ \mathrm{K})$ for (a) $(Lu_{1-x}Y_x)_2Fe_3Si_5$ and $(Lu_{1-x}Dy_x)_2Fe_3Si_5$ and (b) $(Lu_{1-x}Sc_x)_2Fe_3Si_5$.

contribution of the carrier density, and purely sees the variation in the electron mean-free path, the isotropy of $\rho(T)/\rho(300\ \mathrm{K})$ in the single crystal indicates the isotropy of the electron mean-free path. Thus, it is ensured that the normalized resistivity $\rho(T)/\rho(300\ \mathrm{K})$ is a good measure of the electron mean-free path regardless of single crystal and polycrystal in $Lu_2Fe_3Si_5$. Similar to the "absolute" residual resistivities ρ_0^p, ρ_0^c, and ρ_0^{ab}, the normalized residual resistivity $\rho_0/\rho(300\ \mathrm{K})$ in the inset to Fig. 3 tells us that the polycrystalline $Lu_2Fe_3Si_5$ is dirty compared to the single crystal.

On the basis of the isotropic electron mean-free path revealed by the single-crystalline resistivities, we now study the influence of disorder on the superconductivity in $Lu_2Fe_3Si_5$ by investigating the variation in T_c with $\rho_0/\rho(300\ \mathrm{K})$ in the polycrystalline samples. Figures 4(a) and 4(b) depict the normalized resistivity $\rho(T)/\rho(300\ \mathrm{K})$ of nonmagnetic $(Lu_{1-x}Y_x)_2Fe_3Si_5$ and $(Lu_{1-x}Sc_x)_2Fe_3Si_5$ as a function of temperature, respectively. Figure 4(a) also displays $\rho(T)/\rho(300\ \mathrm{K})$ of magnetic $(Lu_{1-x}Dy_x)_2Fe_3Si_5$. It is noteworthy that the small amount of the Lu-site substitution in nonmagnetic $(Lu_{1-x}Y_x)_2Fe_3Si_5$ and $(Lu_{1-x}Sc_x)_2Fe_3Si_5$ rapidly depresses T_c with the systematic increase in the residual resistivity. Here, we would like to comment on the chemical pressure effect on T_c in $Lu_2Fe_3Si_5$. The unit-cell volume variations in Fig. 1 tell us that Y and Sc substitutions for Lu apply negative and positive chemical pressures, respectively. It is noted that T_c of $Y_2Fe_3Si_5$ and $Lu_2Fe_3Si_5$ under hydrostatic pressure exhibits positive and negative pressure coefficients, $dT_c/dp>0$ and $dT_c/dp<0$, respectively.[20] These T_c variations imply that both the negative and the positive pressures might lower T_c in $Lu_2Fe_3Si_5$. However, considering the difference of T_c in $Lu_2Fe_3Si_5$ (6.1 K)$-$$Y_2Fe_3Si_5$ (2.6 K), and $Lu_2Fe_3Si_5-Sc_2Fe_3Si_5$ (4.6 K) the expected decreases in T_c by the chemical pressure for $(Lu_{1-x}Y_x)_2Fe_3Si_5$ and $(Lu_{1-x}Sc_x)_2Fe_3Si_5$ at $x=0.07$ are $\Delta T_c=-0.25$ and -0.1 K, respectively. These values are much smaller than the T_c depression of $(Lu_{1-x}Y_x)_2Fe_3Si_5$ and $(Lu_{1-x}Sc_x)_2Fe_3Si_5$ in Fig. 4; $\Delta T_c=-2.5$ K at $x=0.07$. Thus, we conclude that the rapid T_c depressions of $Lu_2Fe_3Si_5$ in Fig. 4 are dominated by the pair breaking by impurities. And the present results clearly indicate that *the introduction of disorder gives rise to the strong pair breaking in* $Lu_2Fe_3Si_5$. For magnetic $(Lu_{1-x}Dy_x)_2Fe_3Si_5$, T_c is also steeply depressed with the Dy doping. Comparing the Dy- and the Y-doped samples at $x=0.05$, which exhibit almost the same residual resistivities, $T_c=3.8$ K of $(Lu_{0.95}Dy_{0.05})_2Fe_3Si_5$ is a little lower than $T_c=4.2$ K of $(Lu_{0.95}Y_{0.05})_2Fe_3Si_5$. In $(Lu_{1-x}Dy_x)_2Fe_3Si_5$, as evident from Fig. 2, the Dy doping introduces the magnetic scattering potential. Thus the pair breaking in $(Lu_{1-x}Dy_x)_2Fe_3Si_5$ a little stronger than $(Lu_{1-x}Y_x)_2Fe_3Si_5$ is attributed to the magnetic scattering, which is compatible with the spin-singlet pairing in $Lu_2Fe_3Si_5$.[9]

Figure 5 displays nonmagnetic and magnetic impurity effects on T_c in $Lu_2Fe_3Si_5$ (this work) compared with MgB_2.[21] For MgB_2, the T_c depression by nonmagnetic impurities (Zn) is negligibly small while magnetic impurities (Mn) strongly depress T_c, indicative of the *s*-wave pairing. $Lu_2Fe_3Si_5$, on the other hand, exhibits a strong T_c depression with doping regardless of nonmagnetic and magnetic impurities. As already mentioned in conjunction with Fig. 4, T_c of $Lu_2Fe_3Si_5$ is rapidly depressed by nonmagnetic impurities in accordance with the increase in the residual resistivity. Such a disorder-sensitive superconductivity compellingly suggests *the sign reversal of the superconducting order parameter*.

In the sign-reversal order parameter, it is expected that the pair breaking by disorder results in vanishing of T_c at a critical residual resistivity $\rho_0(0)$ in which the electron mean-free path l_0 is on the order of the superconducting coherence length ξ_0 ($l_0 \simeq \xi_0$). The inset to Fig. 5 shows the T_c depression of $Lu_2Fe_3Si_5$ as a function of the normalized residual resistivity $\rho_0/\rho(300\ \mathrm{K})$. The dotted line in this figure is a linear fit to the experimental plots of nonmagnetic

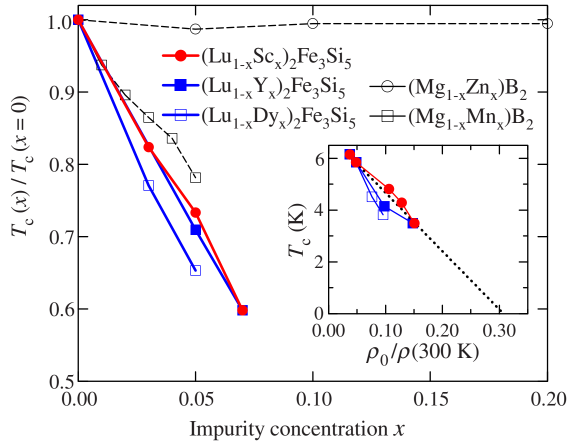

FIG. 5. (Color online) The T_c depression of $Lu_2Fe_3Si_5$ as a function of nonmagnetic (Y,Sc) and magnetic (Dy) impurity concentrations x. Nonmagnetic (Zn) and magnetic (Mn) impurity effects on T_c in MgB_2 (Ref. 21) are displayed for comparison. Inset shows the T_c depression of $Lu_2Fe_3Si_5$ as a function of the normalized residual resistivity $\rho_0/\rho(300\ \mathrm{K})$.

$(Lu_{1-x}Y_x)_2Fe_3Si_5$ and $(Lu_{1-x}Sc_x)_2Fe_3Si_5$. Extrapolating this line to $T_c=0$ expects that the superconductivity disappears at $\rho_0(0)/\rho(300\ K)\simeq 0.3$. For the estimation of the critical residual resistivity $\rho_0(0)$, we assume that the temperature-dependent part of the resistivity, $\Delta\rho(T)=\rho(T)-\rho_0$, is independent of the small amount of the nonmagnetic impurities. And we utilize $\Delta\rho(300\ K)$ of the single-crystalline $Lu_2Fe_3Si_5$ in Fig. 3 for the $\rho_0(0)$ estimation: c-axis $\Delta\rho^c(300\ K)=158\ \mu\Omega$ cm and in-plane $\Delta\rho^{ab}(300\ K)=513\ \mu\Omega$ cm, respectively. Using these $\Delta\rho(300\ K)$ values, $\rho_0(0)/\rho(300\ K)=\rho_0(0)/[\rho_0(0)+\Delta\rho(300\ K)]=0.3$ leads to the critical residual resistivities, c-axis $\rho_0^c(0)=68\ \mu\Omega$ cm and in-plane $\rho_0^{ab}(0)=220\ \mu\Omega$ cm, respectively.

Concerning the in-plane $\rho_0^{ab}(0)=220\ \mu\Omega$ cm, we would like to roughly estimate the corresponding electron mean-free path l_0^{ab} by using the formula $l_0^{ab}=\hbar(3\pi^2)^{1/3}/[e^2n^{2/3}\rho_0^{ab}(0)]$. For $Lu_2Fe_3Si_5$, the in-plane Hall coefficient in low temperatures, $R_H\simeq 1.5\times 10^{-9}\ m^3\ C^{-1}$,[6] leads to $1/R_He\simeq 4.2\times 10^{27}\ m^{-3}$. Substituting this $1/R_He$ value for the carrier density n in the above l_0^{ab} formula calculates $l_0^{ab}\simeq 22$ Å. On the other hand, the upper critical field $\mu_0H_{c2}(0)\simeq 13$ T with $H\parallel c$ in $Lu_2Fe_3Si_5$ (Refs. 6 and 7) calculates the in-plane coherence length $\xi_0^{ab}\simeq 50$ Å. These l_0^{ab} and ξ_0^{ab} are comparable within an order of magnitude, but $l_0^{ab}<\xi_0^{ab}$. We note here that the temperature-dependent R_H in $Lu_2Fe_3Si_5$ is indicative of the multiband feature.[6] In the multiband system, $1/R_He$ is no longer the correct expression for the carrier density and might become larger than the true carrier density when the contributions of electron and hole bands cancel each other in R_H.[22] The smaller l_0^{ab} than ξ_0^{ab} might be attributed to the overestimation of n due to the multiband feature.

The present study provides a strong evidence for the sign reversal of the superconducting order parameter in the multigap structure in $Lu_2Fe_3Si_5$. However, the present study is insufficient to distinguish between the non-s-wave even-parity and the $s_\pm$-wave pairings. Further experiments which probe angle-resolved information, such as magnetothermal experiments with rotating magnetic field, and angle-resolved photoemission spectroscopy should be performed to determine the superconducting gap structure of $Lu_2Fe_3Si_5$.

In summary, we studied the effect of nonmagnetic and magnetic impurities on the superconductivity of $Lu_2Fe_3Si_5$ by small-amount substitution of nonmagnetic Y, Sc, and magnetic Dy for Lu. The rapid T_c depression by nonmagnetic impurities in accordance with the increase in residual resistivity reveals the disorder-sensitive superconductivity in $Lu_2Fe_3Si_5$, providing a strong evidence for the sign reversal of the superconducting order parameter.

We thank T. Baba and Y. Nakajima for helpful comments. This work was partly supported by a Grant-in-Aid for Scientific Research from the Ministry of Education, Culture, Sports, Science and Technology of Japan.

[1] Y. Kamihara, T. Watanabe, M. Hirano, and H. Hosono, J. Am. Chem. Soc. **130**, 3296 (2008).

[2] H. F. Braun, Phys. Lett. A **75**, 386 (1980).

[3] H. F. Braun, in *Ternary Superconductors*, edited by G. K. Shenoy, B. D. Dunlap, and F. Y. Fradin (North-Holland, Amsterdam, 1981), p. 225.

[4] H. F. Braun, C. U. Segre, F. Acker, M. Rosenberg, S. Dey, and P. Deppe, J. Magn. Magn. Mater. **25**, 117 (1981).

[5] D. C. Johnston and H. F. Braun, in *Superconductivity Ternary Compounds II*, edited by M. B. Maple and Ø. Fischer (Springer-Verlag, Berlin, 1982).

[6] Y. Nakajima, T. Nakagawa, T. Tamegai, and H. Harima, Phys. Rev. Lett. **100**, 157001 (2008).

[7] R. T. Gordon, M. D. Vannette, C. Martin, Y. Nakajima, T. Tamegai, and R. Prozorov, Phys. Rev. B **78**, 024514 (2008).

[8] H. J. Choi, D. Roundy, H. Sun, M. L. Cohen, and S. G. Louie, Nature (London) **418**, 758 (2002).

[9] R. J. Noer, T. P. Chen, and E. L. Wolf, Phys. Rev. B **31**, 647 (1985).

[10] C. B. Vining, R. N. Shelton, H. F. Braun, and M. Pelizzone, Phys. Rev. B **27**, 2800 (1983).

[11] Y. Xu and R. N. Shelton, Solid State Commun. **68**, 395 (1988).

[12] H. F. Braun and C. U. Segre, Bull. Am. Phys. Soc. **26**, 343 (1981).

[13] T. Baba, M. Matsunami, R. Eguchi, Y. Ishida, A. Chainani, M. Okawa, K. Ishizaka, T. Kiss, T. Shimojima, H. Sasame, T. Watanabe, Y. Takano, Y. Senba, H. Ohashi, T. Togashi, S. Watanabe, X. Y. Wang, C. T. Chen, and S. Shin (unpublished).

[14] S. Tsuda, T. Yokoya, T. Kiss, T. Shimojima, S. Shin, T. Togashi, S. Watanabe, C. Zhang, C. T. Chen, S. Lee, H. Uchiyama, S. Tajima, N. Nakai, and K. Machida, Phys. Rev. B **72**, 064527 (2005).

[15] Y. Kasahara, T. Iwasawa, H. Shishido, T. Shibauchi, K. Behnia, Y. Haga, T. D. Matsuda, Y. Onuki, M. Sigrist, and Y. Matsuda, Phys. Rev. Lett. **99**, 116402 (2007).

[16] I. I. Mazin, D. J. Singh, M. D. Johannes, and M. H. Du, Phys. Rev. Lett. **101**, 057003 (2008); K. Kuroki, S. Onari, R. Arita, H. Usui, Y. Tanaka, H. Kontani, and H. Aoki, *ibid.* **101**, 087004 (2008).

[17] A. D. Christianson, E. A. Goremychkin, R. Osborn, S. Rosenkranz, M. D. Lumsden, C. D. Malliakas, I. S. Todorov, H. Claus, D. Y. Chung, M. G. Kanatzidis, R. I. Bewley, and T. Guidi, Nature (London) **456**, 930 (2008); G. Mu, H. Luo, Z. Wang, L. Shan, C. Ren, and H. H. Wen, Phys. Rev. B **79**, 174501 (2009); Y. Machida, K. Tomokuni, T. Isono, K. Izawa, Y. Nakajima, and T. Tamegai, J. Phys. Soc. Jpn. **78**, 073705 (2009).

[18] A. V. Balatsky, I. Vekhter, and J. X. Zhu, Rev. Mod. Phys. **78**, 373 (2006).

[19] A. A. Golubov and I. I. Mazin, Phys. Rev. B **55**, 15146 (1997).

[20] C. U. Segre and H. F. Braun, in *Physics of Solids Under High Pressure*, edited by J. S. Schilling and R. N. Sheloton (North-Holland, Amsterdam, 1981), p. 381.

[21] S. Xu, Y. Moritomo, K. Kato, and A. Nakamura, J. Phys. Soc. Jpn. **70**, 1889 (2001).

[22] For instance, the Hall coefficient R_H of a two-band system consisting of electron and hole bands is written as $R_H=(n_h\mu_h^2-n_e\mu_e^2)/[e(n_h\mu_h+n_e\mu_e)^2]$. Here, n_h (n_e) is the carrier density of the hole (electron) band and μ_h (μ_e) is the mobility of the hole (electron) band.